

The vertical structure of Titan's upper atmosphere from Cassini Ion Neutral Mass Spectrometer measurements

Roger V. Yelle^{a,*}, N. Borggren^a, V. de la Haye^b, W.T. Kasprzak^c, H.B. Niemann^c,
I. Müller-Wodarg^d, J.H. Waite Jr.^b

^a Department of Planetary Sciences, University of Arizona, Tucson, AZ 85721, USA

^b Department of Atmospheric, Oceanic Sciences and Space Physics, University of Michigan, Ann Arbor, MI 48109, USA

^c NASA Goddard Space Flight Center, Greenbelt, MD 20771, USA

^d Space and Atmospheric Physics Group, Imperial College London, London SW7 2BW, UK

Received 4 May 2005; revised 25 April 2006

Available online 27 April 2006

Abstract

Data acquired by the Ion Neutral Mass Spectrometer (INMS) on the Cassini spacecraft during its close encounter with Titan on 26 October 2004 reveal the structure of its upper atmosphere. Altitude profiles of N₂, CH₄, and H₂, inferred from INMS measurements, determine the temperature, vertical mixing rate, and escape flux from the upper atmosphere. The mean atmospheric temperature in the region sampled by the INMS is 149 ± 3 K, where the variance is a consequence of local time variations in temperature. The CH₄ mole fraction at 1174 km is 2.71 ± 0.1%. The effects of diffusive separation are clearly seen in the data that we interpret as an eddy diffusion coefficient of $4_{-3}^{+4} \times 10^9 \text{ cm}^2 \text{ s}^{-1}$, that, along with the measured CH₄ mole fraction, implies a mole fraction in the stratosphere of 2.2 ± 0.2%. The H₂ distribution is affected primarily by upward flow and atmospheric escape. The H₂ mole fraction at 1200 km is $4 \pm 1 \times 10^{-3}$ and analysis of the altitude profile indicates an upward flux of $1.2 \pm 0.2 \times 10^{10} \text{ cm}^{-2} \text{ s}^{-1}$, referred to the surface. If horizontal variations in temperature and H₂ density are small, this upward flux also represents the escape flux from the atmosphere. The CH₄ density exhibits significant horizontal variations that are likely an indication of dynamical processes in the upper atmosphere.

© 2005 Elsevier Inc. All rights reserved.

Keywords: Planets; Aeronomy

1. Introduction

The Ion Neutral Mass Spectrometer (INMS) on the Cassini spacecraft measured the altitude profiles of atmospheric constituents as Cassini passed through Titan's upper atmosphere during the close encounter on 26 October 2004. The encounter is referred to as "TA" in Cassini project terminology and this paper and was the first time that the Cassini spacecraft came close enough to Titan to allow direct measurement of the properties of its upper atmosphere. Titan's upper atmosphere is the site of numerous chemical and thermal processes that effect the structure and composition at all levels of the atmosphere. The

INMS data and associated measurements by other particle and field instruments, represent the first in situ sampling of Titan's atmosphere. The in situ data from the INMS provides higher precision on inferred densities, is sensitive to a broader range of atmospheric constituents, and provides better altitude resolution than has previously been possible.

In this paper we concentrate on the vertical distributions of N₂, CH₄, and H₂. These are the 3 most abundant constituents in Titan's upper atmosphere and the densities of each are relatively straightforward to determine from the INMS data. Moreover, analysis of the altitude profiles of densities provides much of the basic information on the structure of Titan's upper atmosphere: N₂ reveals the temperature profile, CH₄ the vertical mixing rate, and H₂ the thermal escape rate. Other aspects of the INMS investigation including the density of minor species,

* Corresponding author.

E-mail address: yelle@lpl.arizona.edu (R.V. Yelle).

the isotopic composition, the properties of waves, and nonthermal escape rates will be dealt with in separate publications.

2. Observations and data reduction

The INMS can be operated in several different modes that are sensitive to ion species, reactive neutral species, or nonreactive neutral species (Waite et al., 2005). The most important goal for this first close encounter was measurement of the mass density of the upper atmosphere in order to assess its affect on the spacecraft. As a consequence, most observations were made in the Closed Source Neutral (CSN) mode that is sensitive to nonreactive neutral constituents. Full characterization of the composition of Titan's atmosphere is planned for later encounters. Interspersed with the CSN measurements were observations whose primary purpose was to verify instrument tuning and calibration. In this paper we concentrate exclusively on the CSN measurements.

The CSN mode of the INMS utilizes an enhancement chamber wherein the high velocities of atmospheric molecules relative to the spacecraft are converted to thermal velocities through collisions with the walls of the chamber, thereby enhancing the density in the chamber and the effective sensitivity of the INMS. Because of the randomizing nature of the wall collisions, the angular response of the INMS in CSN mode is quite broad, varying essentially as the cosine of the angle between the INMS axis and the spacecraft velocity. As shown in Fig. 1, the spacecraft orientation permitted INMS observations roughly ± 5 min around closest approach and was optimized for INMS measurements from -250 s before closest approach to closest approach. After closest approach the S/C slowly rolled away from the INMS-optimized orientation in order to make radar observations of the surface. The angle between the S/C velocity and the INMS axes reached 25° at $+300$ s. The spacecraft speed relative to Titan varied from 6.06 km s^{-1} at closest approach to 5.86 km s^{-1} on inbound and outbound asymptotes.

Fig. 1 also provides an overview of the geometry of the encounter and some numerical values are listed in Table 1. Closest approach occurred at northern mid-latitudes and near to the dusk terminator: inbound observations are primarily in the sunlit hemisphere and outbound observations in darkness. The spacecraft latitude during the encounter is relatively constant, but the local time varied significantly. Taking 1550 km as the top of the region of interest for this paper, the spacecraft latitude varied between 28 and 42° north latitude and the local time from 3 to 7 PM . Thus, the atmosphere was sampled over a vertical distance of $\sim 400 \text{ km}$ and a horizontal distance of $\sim 3000 \text{ km}$. The relatively inert species discussed here are not affected by chemical sources or sinks that vary with latitude or local time, but latitudinal and local time variations may be caused by dynamical processes (Müller-Wodarg and Yelle, 2002; Müller-Wodarg et al., 2003). Calculations imply that these variations are on the order of 10 – 30% . The vertical variations in density are much larger. In the discussion that follows, we first analyze the measurements in terms of vertical variations before discussing the importance of horizontal variations.

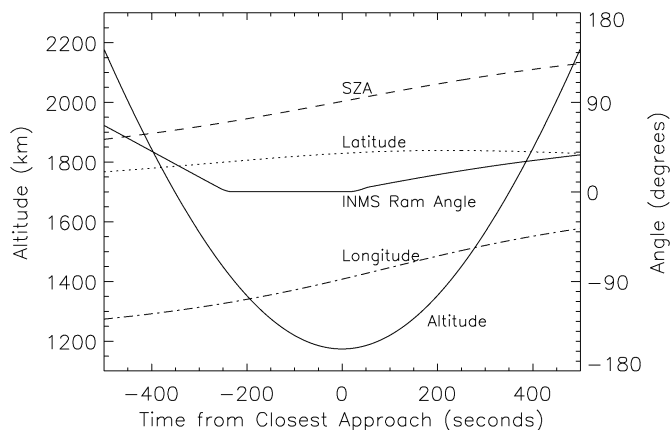


Fig. 1. The geometry of the TA encounter.

Table 1
Encounter geometry

Quantity	Value at closest approach
Time	2004-300T15:30:05
Altitude	1174 km
S/C velocity rel. Titan	6.06 km/s
Latitude	38.6°
Longitude	-87.6°
Local solar time	16.75 h
Solar zenith angle	90.9°

Several corrections are required before the counts measured by the INMS can be converted to number densities. As mentioned above, the CSN observations are interleaved with calibration measurements. Upon examination of the data acquired during TA it was discovered that slight changes in the way that voltages were assigned in atmospheric observations made immediately after the calibration observations affected the atmospheric measurements. In one mode the voltages are set from a table of stored values and in another from flight software and, though the values are nominally equal, very slight differences between these two settings are responsible for a change in sensitivity. This is illustrated in Fig. 2 which shows a quasiperiodic anomalous depression in count rates, at the level of about 10% that is perfectly correlated with value of the software flag that controls how voltage are assigned. In order to correct the anomalous data points we fit the log of the count rate outside the problematic region with a fourth-order polynomial in time. We then compare the average value of the data and polynomial fit in the problem region and scale the data by ratio of these values to bring it into line with the nearby measurements.

The next step in the analysis is conversion of count rate to number density. Channel 28 provides the most direct measurement of the N_2 density, but, as shown in Fig. 3, the signal becomes saturated at altitudes below $\sim 1350 \text{ km}$. As discussed in Waite et al. (2005), the INMS has two detectors. The high gain detector is most sensitive and provides most of the data discussed in this report; the low gain detector is designed to provide measurements when the high gain detector is saturated. Fig. 3 shows both high and low gain measurements and, although the N_2 is clearly measured, the statistical uncertainties

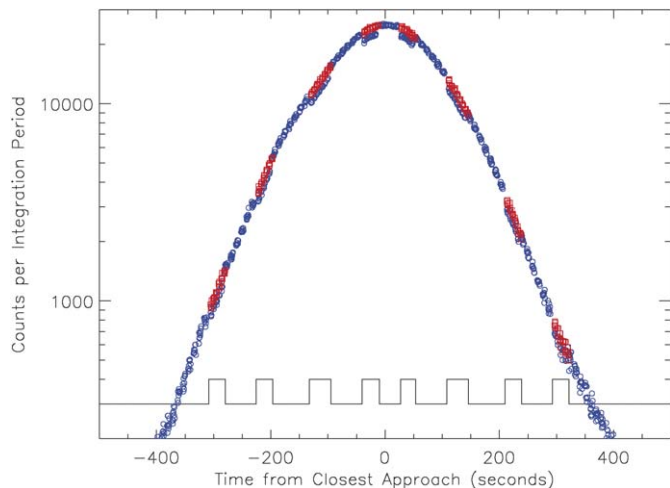


Fig. 2. The count rate in channel 16 as a function of time. The blue circles show the original values and the red squares the corrected values. The square wave reflects the value of a software flag that determines the method for setting INMS voltages and demonstrates that the $\sim 10\%$ depressions in count rate are correlated with the INMS voltage settings.

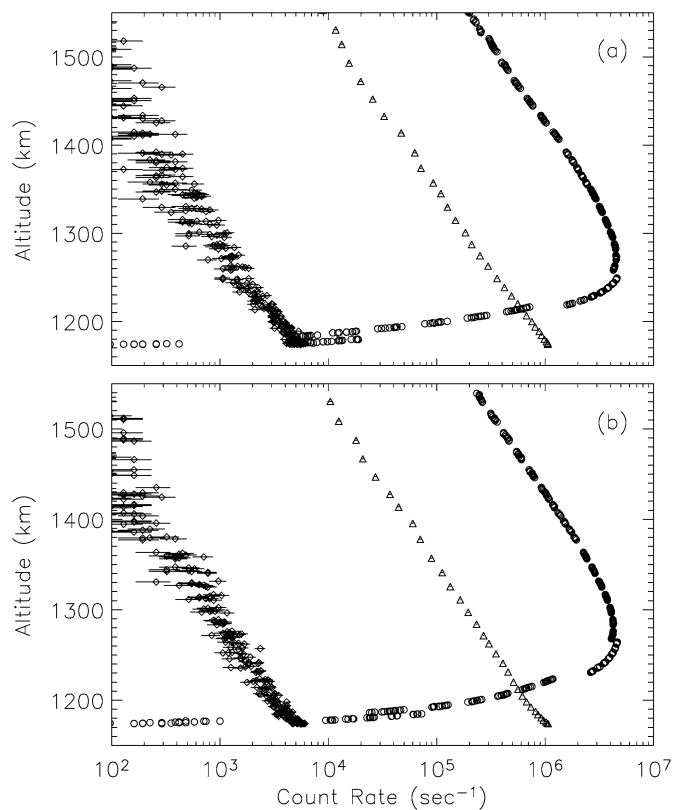


Fig. 3. The count rate for the high gain detector and channel 28 (circles), the high gain detector and channel 14 (triangles) and the low gain detector and channel 28 (diamonds). Channel 28 in the high gain detector exhibits saturation below altitudes of ~ 1350 km. Channel 14 and 28 are parallel at altitudes free of saturation. The upper panel (a) is for inbound observations, the lower panel (b) for outbound.

in the low gain measurements are relatively large. N_2 also produces a large signal in channel 14 which, as shown in Fig. 3, is parallel to that in channel 28 at high altitudes but is not affected by saturation at low altitudes. The SNR for channel 14 is

Table 2
INMS sensitivity^a

Mass channel	N_2	CH_4	H_2
2	–	2.26×10^{-5}	4.96×10^{-3}
14	6.31×10^{-4b}	1.63×10^{-3}	–
16	–	2.90×10^{-2}	–
28	3.20×10^{-2}	–	–
CSN enhancement factor	50.9	38.5	13.6

^a All values are counts $cm^3 s^{-1}$. CSN enhancement factors assume a spacecraft velocity of 6.06 km/s along the INMS axis.

^b Scaled from laboratory value by 1.27.

much higher than that for the low gain detector data for channel 28 and we therefore use channel 14 to determine the N_2 density. However, several corrections are required before the N_2 density can be determined from channel 14. First, CH_4 may also contribute to the signal level in this channel. The count rate in channel 16 at 1174 km is $799,781$ counts s^{-1} , which is due exclusively to CH_4 . Using the data in Table 2 we estimate a corresponding count rate in channel 14 due to CH_4 of $44,788$ counts s^{-1} , which is 5% of the actual count rate in channel 14. Thus, $\sim 95\%$ of the counts in channel 14 are due to N_2 and, although it is necessary to correct for the CH_4 counts, the correction is small and well-determined.

There is a further problem though because, using the pre-flight laboratory calibration data, the N_2 density implied by the count rate in channel 14 is 27% higher than that implied by channel 28. This comparison refers to the 1400–1600 km region where saturation is not a concern and the two channels should give consistent results. The most likely explanation for this is a change in the INMS sensitivity to N_2 at channel 14. These counts are, of course, produced by N^+ created by dissociative ionization of N_2 . This process imparts the dissociation fragments with excess kinetic energy that may affect the way that the fragment ions are transmitted through the ion optics of the INMS. Thus, any change in the INMS optics during cruise would appear primarily in the sensitivity for dissociation products with significant kinetic energies. This is a well-known effect in mass spectrometers. Comparison of channels 14 and 28 in the 1400–1600 km region imply that the sensitivity for channel 14 has increased by a factor of 1.27 relative to the pre-launch calibration. We therefore scale the channel 14 sensitivity by this factor to force agreement with the N_2 density inferred from channel 28 in the 1400–1600 km region and to extrapolate to the lower altitudes where channel 28 suffers from saturation.

The H_2 density is determined through the count rate in channel 2. As shown in Table 2, CH_4 also contributes to the count rate in channel 2, but again, the relative contribution and required correction are small. The measured count rates and calibration data imply that CH_4 contributes 3% of the count rate for channel 2. Unfortunately, determination of the H_2 density is complicated by another effect. Fig. 4 shows that the channel 2 count rate frequently exhibits large excursions from the mean value and that these anomalous measurements are correlated with thruster firings. The spacecraft thrusters operate with hydrazine (N_2H_4) and H_2 is a significant component of the thruster effluent. The high channel 2 count rates above

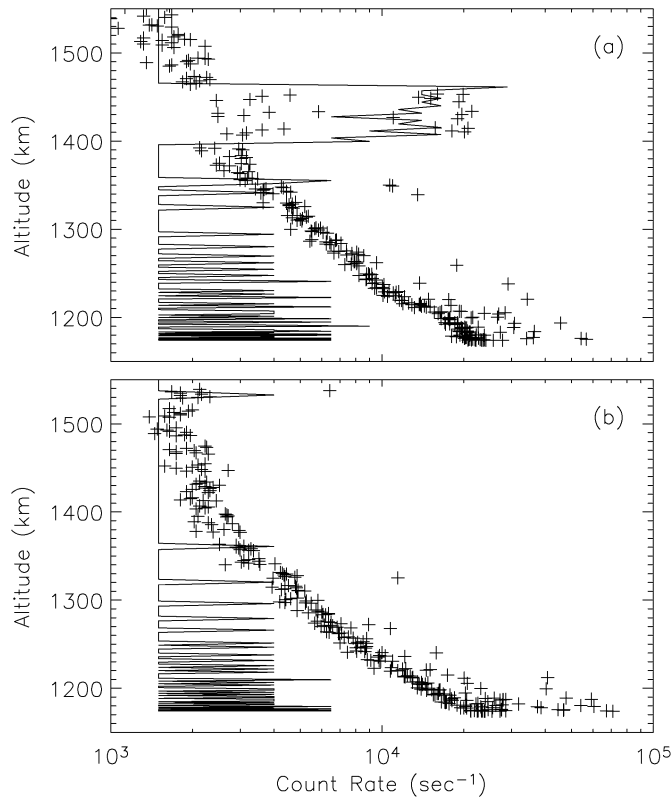


Fig. 4. The count rate for the high gain detector and channel 2. The information on thruster operations relayed to ground consists of accumulated thruster operation time on 2 s intervals. Each thruster firing nominally lasts 0.125 s. and from this we calculate the number of thruster firings in each 2 s interval. This is shown as the solid line in the diagram. The scale is arbitrary and shows only when thruster firings occur. The upper panel (a) is for inbound observations, the lower panel (b) for outbound.

1400 km on the inbound leg are correlated with the thruster firing from 254 to 224 s prior to closest approach that stopped the spacecraft rotation with the INMS axis in the spacecraft ram direction. Aside from this maneuver though thruster firings are relatively rare above ~ 1200 km and are easily recognized. Near closest approach, the thrusters are firing often in order to offset the torque on the spacecraft due to atmospheric drag and channel 2 signal levels at altitudes below ~ 1250 km are unreliable. The N_2 measurements are not affected by the thruster firings because the contamination from the thrusters is small compared with the larger N_2 density in Titan's atmosphere.

The CH_4 density is determined through the count rate in channel 16. This is the most straightforward of the species densities to compute because channel 16 is not significantly affected by any other species, is not saturated, and is not contaminated by thruster emissions.

3. Implications

Fig. 5 shows the N_2 , CH_4 , and H_2 density versus altitude for inbound and outbound legs. Several interesting characteristics can be seen directly from examination of the profiles. At high altitudes there are clear differences between the N_2 , CH_4 , and H_2 scale heights indicating the importance of diffusive separa-

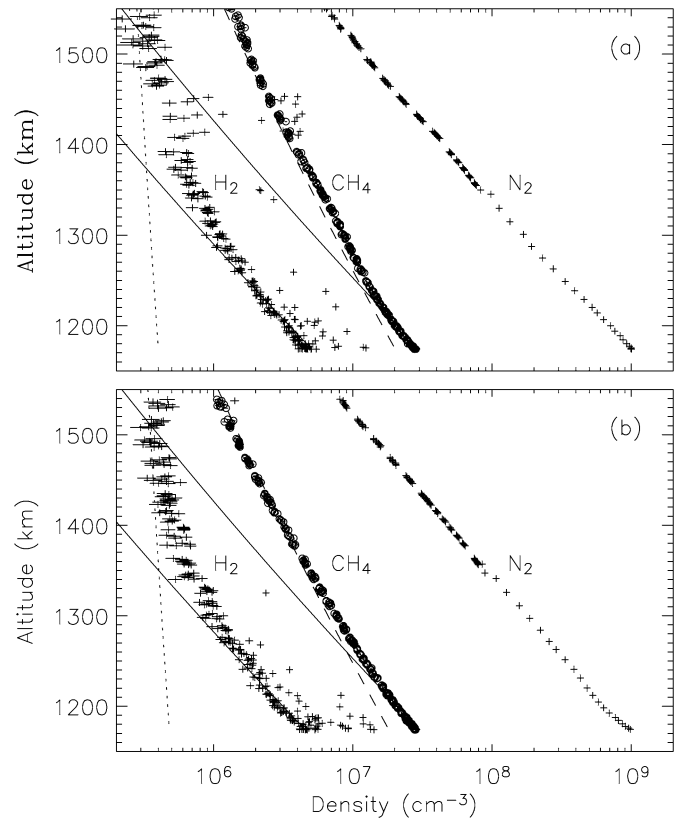


Fig. 5. The number density of N_2 , CH_4 , and H_2 as a function of altitude for inbound (a) and outbound (b) legs. The dashed and dotted lines represent hydrostatic equilibrium distributions for the CH_4 and H_2 molecular masses for an isothermal atmosphere at 149 K. The solid lines have the same slope as a hydrostatic N_2 distribution but are normalized to the CH_4 and H_2 measurements. At low altitudes, the observed CH_4 and H_2 distributions have slopes similar to that of N_2 , but adopt their own scale heights at high altitudes.

tion in this part of the atmosphere. However, the N_2 and CH_4 distributions become more nearly parallel at low altitude, indicating the importance of vertical mixing in the atmospheric region near 1200 km. The H_2 density profile remains parallel to the N_2 profile to higher altitudes than does the CH_4 profile. This is the signature of a large upward flux, as expected for H_2 , because of its rapid escape rate from the top of the atmosphere. We analyze these aspects of the data below, by first constructing a model for the variation of mass density and mean molecular weight with altitude. This allows determination of the temperature and enables estimates of the escape flux from the atmosphere.

We compute the mean molecular weight of the atmosphere assuming that N_2 and CH_4 are the only important species. As shown in Fig. 5, the H_2 density is more than two orders of magnitude less than the N_2 density and can safely be ignored. The mean molecular weight in the hydrostatic equilibrium calculations is computed from solution of the diffusion equation for a binary gas mixture in a gravitational field. At the highest altitudes considered here the CH_4 density is roughly 20% that of N_2 and the usual assumption of a minor species diffusing through a stationary background gas is not applicable. The general equation for diffusion of two species of comparable density

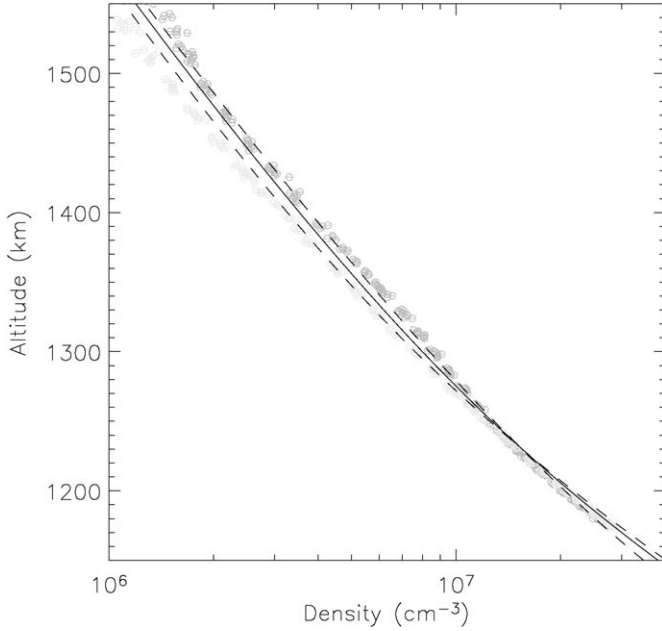


Fig. 6. The CH_4 density for inbound (blue) and outbound (red) legs. The solid line represents a diffusive equilibrium model with constant eddy diffusion coefficient of $K = 4 \times 10^9 \text{ cm}^2 \text{ s}^{-1}$. The dashed lines represent models for $K = 1 \times 10^9$ (upper curve) and $8 \times 10^9 \text{ cm}^2 \text{ s}^{-1}$ (lower curve).

can be written as

$$\Phi_i = -(\widetilde{D}_{ij} + K)N \frac{\partial X_i}{\partial r} - \widetilde{D}_{ij}N \frac{(m_i - m_j)g}{kT} X_i(1 - X_i), \quad (1)$$

where Φ_i is the flux, X_i the mole fraction, and m_i the mass of the i th constituent, N is the total number density, K is the eddy diffusion coefficient, g is gravitational acceleration, and T is temperature. The thermal diffusion terms have been neglected because, as shown below, Titan's upper atmosphere appears isothermal in the altitude range under consideration. The variable \widetilde{D}_{ij} is related to the diffusion coefficient, D_{ij} through $\widetilde{D}_{ij} = D_{ij}/(1 - (1 - m_i/m_j)X_i)$. Equation (1) is derived in Appendix A. Diffusion coefficients for CH_4 and H_2 in N_2 are obtained from Mason and Marrero (1970).

Figs. 6 and 7 show the CH_4 density and mean molecular weight of the atmosphere along with models computed according to Eq. (1) with $\Phi = 0$. The best fit to the combined set of inbound and outbound data has $K = 4 \times 10^9 \text{ cm}^2 \text{ s}^{-1}$; however there are obvious variations with inbound densities significantly larger than outbound. The inbound data when considered alone is best fit by with $K = 1 \times 10^9 \text{ cm}^2 \text{ s}^{-1}$ and the outbound data with $K = 8 \times 10^9 \text{ cm}^2 \text{ s}^{-1}$. The difference in inbound/outbound results is a reflection of horizontal variations in the CH_4 abundance. Local time variations in the CH_4 density can be caused by the interplay of dynamical and diffusive processes in Titan's upper atmosphere (Müller-Wodarg and Yelle, 2002), but the observed variation is opposite to that expected for a solar-driven circulation. This may indicate the importance of additional energy or momentum sources in the upper atmosphere, such as precipitating energetic particles from the magnetosphere or atmospheric waves, but more data and further modeling are required to assess these possibilities.

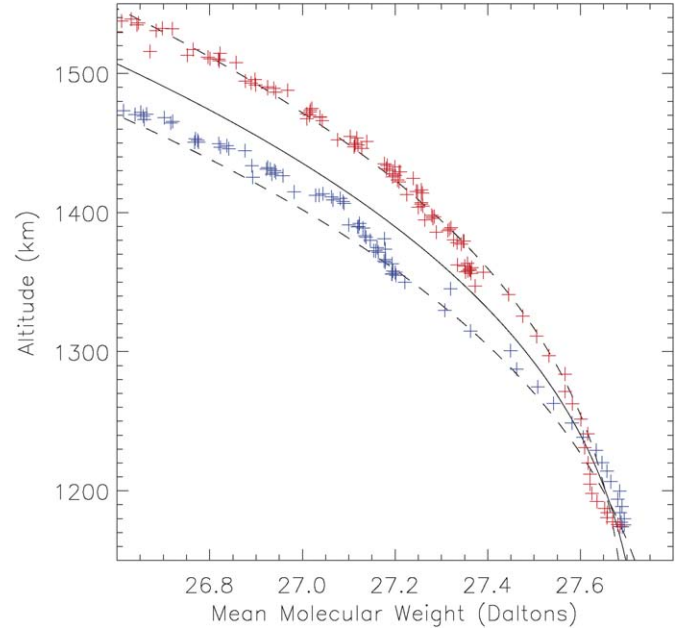


Fig. 7. Mean molecular weight versus altitude and 3 models. The solid line represents a diffusive equilibrium model with constant eddy diffusion coefficient of $K = 4 \times 10^9 \text{ cm}^2 \text{ s}^{-1}$. The dashed lines represent models for $K = 1 \times 10^9$ (lower curve) and $8 \times 10^9 \text{ cm}^2 \text{ s}^{-1}$ (upper curve).

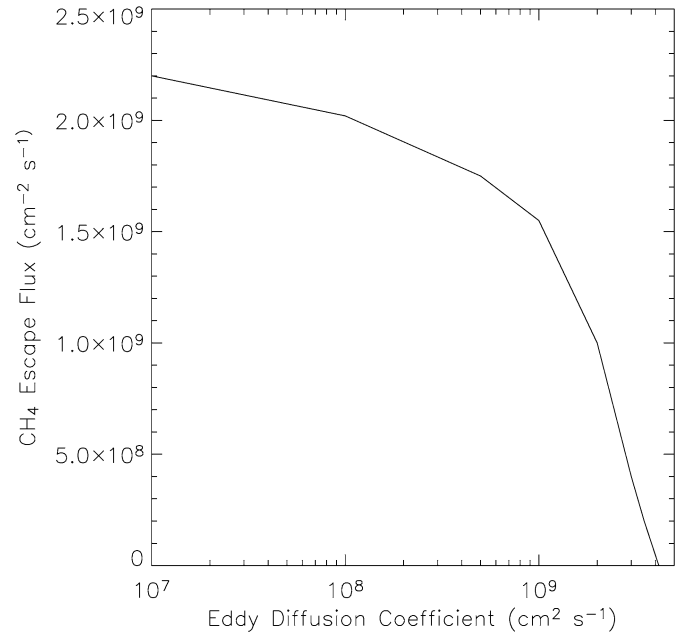


Fig. 8. The combination of eddy diffusion coefficient and CH_4 escape flux that provide a good fit to the data.

The measured CH_4 profile can also be fit with models for a nonzero flux and smaller eddy diffusion coefficients. This is because eddy diffusion and upward flow both drive the CH_4 profile toward a well-mixed profile. The measured N_2 and CH_4 densities show that CH_4 is well mixed to approximately 1200 km. Fig. 8 shows the combinations of K and Φ that provide a good match to the set of inbound and outbound data. For small values of K an upward value of $\Phi = 2.2 \times 10^9 \text{ cm}^{-2} \text{ s}^{-1}$ is sufficient in itself to keep the CH_4 profile well mixed to

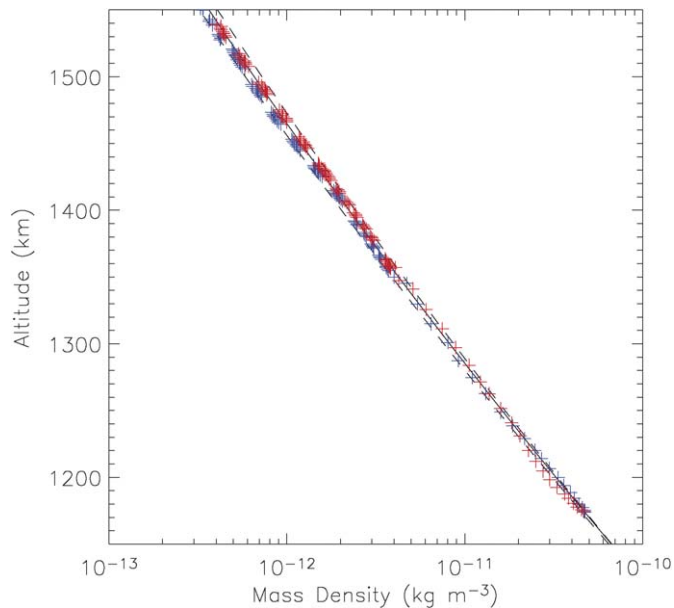


Fig. 9. Mass density versus altitude and isothermal models with temperatures of 149 (solid curve), 152 (upper dashed curve), and 146 (lower dashed curve).

1200 km. For large values of K , only a small or zero upward flux is required to match the observed profiles. The CH_4 flux, if it is real, is not due to photolysis. Although CH_4 must flow upward to replenish the CH_4 destroyed by photolysis, the column-integrated photolysis rate and the upward flux in the region of interest is of order $10^7 \text{ cm}^{-2} \text{ s}^{-1}$, which is too small to have a significant effect on the CH_4 density profile. A nonzero upward flux of CH_4 at the location of the measurements could be due to latitude or local time transport processes or to rapid escape of CH_4 from Titan. These possibilities are discussed in the next section.

The diffusion models also provide the CH_4 mole fraction deep in the atmosphere. The measured value at 1174 km is $2.7 \pm 0.1\%$. By extrapolating this value to lower altitudes using the diffusion models we find that the $K = 4 \times 10^9$, 1×10^9 , and $8 \times 10^9 \text{ cm}^2 \text{ s}^{-1}$ models imply a mole fractions in the deep atmosphere of 2.2%, 2.0%, and 2.4%, respectively. These values are in good agreement with the value of $1.6 \pm 0.5\%$ determined by Flasar et al. (2005) from analysis of CH_4 infrared emissions from Titan.

Armed with a model for the mean molecular weight, we can calculate the altitude profile of mass density. Fig. 9 shows hydrostatic equilibrium models for isothermal atmospheres at temperatures of 149, 146, and 152 K, corresponding to eddy diffusion coefficients of $K = 4 \times 10^9$, 1×10^9 , and $8 \times 10^9 \text{ cm}^2 \text{ s}^{-1}$, respectively. The data is well matched by the isothermal models, leading us to conclude that there is no evidence for a temperature gradient in the 1150–1550 km region of the atmosphere. The higher temperature model provides the best fit to the outbound data and the lower temperature model the best fit to the inbound data. Thus, there appears to be a $\sim 5 \text{ K}$ temperature variation over the 4 h in local time covered by the observations, but, paradoxically, the nighttime temperatures appear higher than the daytime temperatures.

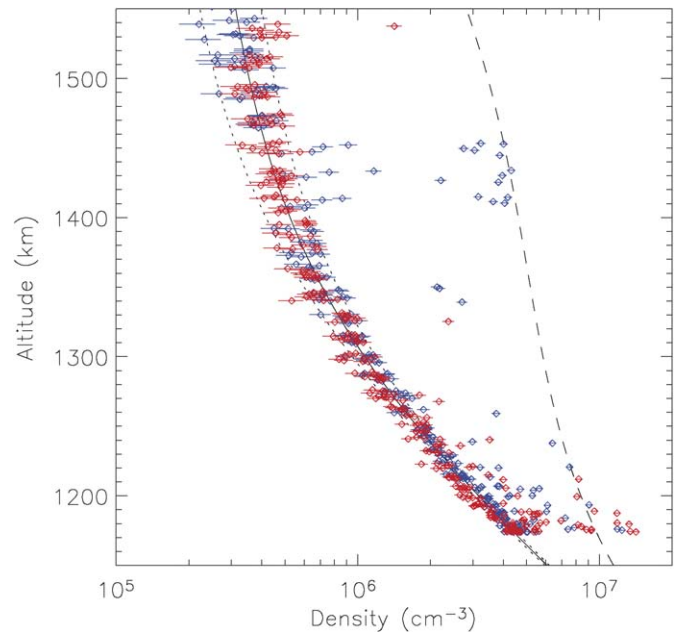


Fig. 10. Comparison of the H_2 density and models based on diffusion and escape. All models assume an H_2 mole fraction at deeper levels of 4×10^{-3} and an eddy diffusion coefficient of $4 \times 10^9 \text{ cm}^2 \text{ s}^{-1}$. The solid line shows a model for an upward flux of $\Phi = 1.2 \times 10^{10} \text{ cm}^{-2} \text{ s}^{-1}$. The two dotted lines show results for 1.0×10^{10} and $1.4 \times 10^{10} \text{ cm}^{-2} \text{ s}^{-1}$, illustrating the fact that the flux is determined to good accuracy from the density profile. The dashed line shows a model for an upward flux equal to the Jeans escape flux of $\Phi_j = 3.6 \times 10^9 \text{ cm}^{-2} \text{ s}^{-1}$.

Close examination of Figs. 6 and 7 reveals periodic variations about the mean values of density and mean molecular weight, as represented by the models. This is evidence for waves in Titan's upper atmosphere. The characteristics of these waves are not investigated here, we simply note that the apparent horizontal variation in temperature may be related to the periodic vertical variations.

H_2 is well mixed to higher levels than CH_4 , indicating a large upward flux. Fig. 10 shows the measured H_2 density and models, calculated by solving Eq. (1), for several values of Φ . The models use the values of $T = 149 \text{ K}$ and $K = 4 \times 10^9 \text{ cm}^2 \text{ s}^{-1}$ determined from the analysis of the N_2 and CH_4 profiles described above. The best fit to the H_2 density profile is achieved with a mole fraction at 1150 km of $X = 4 \times 10^{-3}$ and an upward flux at that level of $\Phi = 5.8 \pm 0.1 \times 10^9 \text{ cm}^{-2} \text{ s}^{-1}$, which is equal to the limiting flux at that altitude. The corresponding escape flux, referred to the surface, is $1.2 \pm 0.2 \times 10^{10} \text{ cm}^{-2} \text{ s}^{-1}$. The Jeans escape flux is equal to $1.7 \times 10^9 \text{ cm}^{-2} \text{ s}^{-1}$ at 1150 km or $3.6 \times 10^9 \text{ cm}^{-2} \text{ s}^{-1}$, referred to the surface. The discrepancy between the upward flux inferred from the H_2 profile and the Jeans escape flux is discussed further in the next section.

4. Discussion and summary

The primary results from analysis of the N_2 , CH_4 , and H_2 density profiles are:

- (1) The thermal structure of Titan's upper atmosphere is well characterized as isothermal with a temperature of $T =$

- 149 ± 3 K. There appears to be a ~ 5 K variation in local time with evening temperatures hotter than afternoon temperatures.
- (2) The CH_4 mole fraction at 1174 km is $2.71 \pm 0.1\%$ and the H_2 mole fraction at 1174 km is 4×10^{-3} .
 - (3) The CH_4 profile can be matched by various combinations of eddy diffusion and upward flux, as shown in Fig. 8. The eddy coefficient derived assuming a negligible upward flux is $K = 4_{-3}^{+4} \times 10^9 \text{ cm}^2 \text{ s}^{-1}$.
 - (4) Using the values above for the CH_4 mole fraction and eddy diffusion coefficient implies a CH_4 mole fraction in Titan's stratosphere of $2.2 \pm 0.2\%$.
 - (5) The upward flux of H_2 referred to the surface, is $1.2 \pm 0.2 \times 10^{10} \text{ cm}^{-2} \text{ s}^{-1}$, significantly larger than the Jean escape flux of $3.6 \times 10^9 \text{ cm}^{-2} \text{ s}^{-1}$.

Previously, Smith et al. (1982) determined the temperature of Titan's upper atmosphere through analysis of the Voyager 1 UV solar occultation experiment of 176 ± 20 K for the ingress data and 196 ± 20 K for the egress data. The ingress data was of higher quality than the egress data and 176 K is the value found most often in the literature and has been used in numerous studies of chemistry and physical conditions in Titan's upper atmosphere. Recently however, Vervack et al. (2004) reanalyzed the Voyager occultation data and determined a temperature of 153 ± 5 K, in excellent agreement with the value of 149 ± 3 K found here. Both the Vervack et al. (2004) value and that reported here refer to the equatorial region near the terminator and local time and latitudinal variations should not affect the comparison. It is remarkable that these two measurements, made 23 years apart, should agree so well. The Voyager 1 encounter with Titan occurred near the maximum of solar cycle 21 while the Cassini encounter occurred during the descending phase of solar cycle 23. The F10.7 flux at the time of the encounters were 257 for Voyager 1 and 130 for Cassini. The SOLAR2000 proxy models (Tobiska, 2004) for the solar EUV flux imply a net EUV flux below 800 Å of 0.9 and 0.3 $\text{erg cm}^{-2} \text{ s}^{-1}$, respectively, at 1 AU. Thus, the solar output at the time of the Voyager 1 encounter was more than a factor of two larger during the Voyager 1 encounter than during the Cassini TA encounter; nevertheless, the temperature of the upper atmosphere was unchanged within measurement error.

Yelle (1991) argued that the temperature of Titan's upper atmosphere is controlled by the balance between solar heating and radiative cooling by HCN and also suggested that variations in radiative cooling by HCN should partly cancel variations in solar heating, preventing large temperature variations in the upper atmosphere. The lack of change in upper atmospheric temperature between the Voyager 1 and Cassini eras may be evidence for this feedback but further monitoring and simultaneous measurements of the temperature and HCN density, planned for later in the Cassini mission, will address this question. The possible role of large waves in the thermospheric energy balance must also be considered.

The CH_4 mole fraction in Titan's upper atmosphere reported here is also in excellent agreement with the value determined by Vervack et al. (2004). These authors found a mole fraction

of approximately 2.4% in the 950–1150 km region, just below that probed by the INMS measurements. The Voyager 1 egress data implied a mole fraction of 1.1%, but again, Vervack et al. (2004) did not view the egress data as reliable as the ingress data. The mole fraction in the stratosphere implied by INMS measurements and the diffusive equilibrium models are in good agreement with that determined by Flasar et al. (2005) for CIRS observations of CH_4 emissions.

The H_2 mole fraction inferred here is substantially larger than the value of 1×10^{-3} determined by Samuelson et al. (1997) from analysis of Titan's IR spectrum. The Samuelson et al. (1997) analysis constraint the H_2 mole fraction in the troposphere, so the difference could be due to altitude variations in the H_2 mole fraction. The models of Lebonnois et al. (2003) show a $\sim 50\%$ increase in the H_2 mole fraction from the troposphere to the mesosphere. There may also be systematic differences between the IR spectroscopy and mass spectroscopy determinations. Analysis of Cassini/Huygens GCMS data and CIRS observations should shed light on the matter.

The INMS measurements are in the altitude region where the CH_4 profile is changing from fully mixed to diffusively separated. If, for the moment, we assume a negligible CH_4 escape flux and equate the molecular diffusion coefficient for CH_4 and N_2 to the eddy diffusion coefficient we derive a homopause altitude of 1200 km. This is an extremely high altitude, only several scale heights below the exobase. This eddy diffusion coefficient is an order of magnitude or more larger than found in any other atmosphere in our Solar System. The result is not new (Strobel et al., 1992; Vervack et al., 2004) but has not been universally accepted, perhaps due to the difficult nature of the Voyager UV occultations and the fact that the value is so high. The only alternative explanation is that CH_4 is escaping at close to the diffusion-limited rate; however, as we discuss below, this hypothesis is also problematic. Regardless of whether eddy diffusion of diffusion-limited flow is affecting the altitude profile, CH_4 does remain mixed to high altitudes.

We use the term “eddy diffusion coefficient” here in the restricted sense of a parameter used to model the altitude profile of a minor species. Whether the eddy diffusion coefficient represents true mixing or is a manifestation of other processes, such as global circulation, remains an open problem whose solution requires a more comprehensive measurement set than currently available. Note that the approach followed here is identical to that of earlier studies of eddy diffusion in Titan's upper atmosphere (Smith et al., 1982; Strobel et al., 1992; Vervack et al., 2004) and our results are directly comparable.

Müller-Wodarg and Yelle (2002) have shown that the persistence of a well mixed CH_4 profile to high levels in the atmosphere may be related to the circulation of the upper atmosphere. Essentially, this is a consequence of vigorous dynamics in Titan's upper atmosphere, coupled with the large extent of the atmosphere, which enhances vertical motions relative to horizontal. Müller-Wodarg and Yelle (2002) estimate an eddy diffusion coefficient due to global circulation of $10^9 \text{ cm}^2 \text{ s}^{-1}$, toward the low end of the values inferred from the data. The problem with applying this approach to analysis of the INMS data is that the dynamical calculations in Müller-

Wodarg and Yelle (2002) are based on solar driven flow which is clearly at odds with horizontal variations evident in the INMS measurements. A more vigorous circulation than calculated by Müller-Wodarg and Yelle (2002) would cause more mixing of the upper atmosphere. The fact that the observed horizontal variations in CH₄ and the observed temperature variations are opposite to that implied by the dynamical models also support this hypothesis because, presumably, additional energy or momentum sources in the upper atmosphere, required to explain the CH₄ and temperature variations, would contribute to the vertical mixing rate. It is also possible that the circulation of the upper atmosphere could alter the CH₄ profile locally, in a manner that mimics mixing, but again investigation of this hypothesis requires a more comprehensive data set.

The upper atmospheric temperature, CH₄ distribution, and the eddy diffusion coefficient reported here differ substantially from that employed in most modeling studies of Titan's upper atmosphere. The CH₄ in the upper atmosphere is close to that for the stratosphere, whereas photochemical models have adopted much larger CH₄ mole fractions, of order 10%, in the photochemical region (Yung et al., 1984; Toubanc et al., 1995; Lara et al., 1996; Wilson and Atreya, 2004). If the eddy diffusion explanation of the CH₄ profile is correct then the eddy diffusion coefficient in the upper atmosphere adopted in these studies is far too small, and this will strongly affect the altitude profile of photochemical species. The next generation of photochemical models should employ substantially different assumptions than pre-Cassini models.

The discrepancy between the upward flux inferred from analysis of the H₂ density profile and the Jeans escape flux has two possible explanations. In the general case, the upward flux at a specific latitude and longitude is equal to the sum of the escape flux and the ballistic flux from the exobase, which may be either positive or negative and represents transport from one location to another through ballistic flow in the exosphere. This flow is driven by variations in temperature and H₂ density at the exobase. The difference between the inferred escape flux and the Jeans escape flux is roughly $8 \times 10^9 \text{ cm}^{-2} \text{ s}^{-1}$. We can make a rough estimate of the horizontal temperature gradients required to produce a flux of this magnitude by assuming that the H₂ density is constant with latitude and local time and that the downward flux of H₂ molecules at the exobase is characterized by a Maxwell–Boltzmann distribution at a temperature smaller than the 149 K that characterizes the upward directed molecules. An average temperature of 79 K for the downward directed molecules is necessary to explain an upward flux of $8 \times 10^9 \text{ cm}^{-2} \text{ s}^{-1}$. This represents a lower limit to the required temperature difference because the H₂ density at the exobase will adjust to the temperature difference and densities should be small where temperatures are large, decreasing the imbalance in fluxes. It seems extremely unlikely that there are horizontal temperature differences this large in Titan's upper atmosphere. We therefore conclude that the upward flux inferred from the H₂ density profile represents primarily an escape flux.

The difference between the inferred escape flux and the Jeans escape flux indicates that nonthermal processes play a dominant role in the escape of H₂ from Titan. Nonthermal es-

cape processes dominate over thermal escape in most Solar System atmospheres (Hunten, 1982) but H₂ on Titan was thought to be an exception because thermal escape is so rapid (Bertaux and Kockarts, 1983; Lebonnois et al., 2003). Possible nonthermal escape mechanisms include charge-exchange, sputtering, or ion pick-up.

Loss due to charge exchange occurs when a collision between an energetic ion and a thermal neutral produces an energetic neutral that has a high probability of escaping the atmosphere. The escape rate from charge-exchange requires the presence of a hot topside ionosphere and should be approximately proportional to the column abundance of H₂ above the exobase. Using the values of density and temperature quoted above, we calculate an H₂ vertical column abundance above 1550 km of $4 \times 10^{13} \text{ cm}^{-2}$. A loss rate above the exobase of $2 \times 10^{-4} \text{ s}^{-1}$ is required to produce a nonthermal escape flux of $8 \times 10^9 \text{ cm}^{-2} \text{ s}^{-1}$. H₂ may also be lost from Titan through ionization above the ionopause followed by pick-up by Saturn's magnetic field. Because the ionopause is usually above the exobase, the ionization rate must be even larger than estimated above for charge exchange because the pick-up ionization acts on a smaller column of H₂. Of course, it is possible, and perhaps likely, that both processes contribute to the nonthermal escape rate. Sputtering occurs when collisions with energetic ions precipitating from the magnetosphere create a splash of ambient molecules, some of which have escape velocity. Shematovich et al. (2003) estimate an N escape rate from this process of $4.3 \times 10^7 \text{ cm}^{-2} \text{ s}^{-1}$. It seems unlikely that sputtering could be responsible for the large H₂ escape rate if the Shematovich et al. estimates are correct, since H₂ is far less abundant than N₂ in Titan's upper atmosphere. However, the Shematovich et al. (2003) estimates are based on Voyager energetic particle data and the more complete measurements available from Cassini may alter these conclusions.

Regardless of the mechanism, the observed upward flux of H₂ provides a good constraint on the CH₄ destruction rate in the atmosphere. There have been several studies of the loss of H₂ from Titan (Hunten, 1973; Bertaux and Kockarts, 1983; Lebonnois et al., 2003) and its connection to photochemistry, but the emphasis in each study has been on thermal escape, because thermal escape of H₂ on Titan is so rapid that it seemed unlikely that nonthermal processes could compete. According to a recent photochemical model by Wilson and Atreya (2004), the CH₄ destruction rate is roughly 50% larger than the H₂ production rate; thus, the net destruction rate of CH₄ is 1.3×10^{28} molecules/s and the lifetime of the total CH₄ reservoir on the atmosphere is 4×10^7 years, assuming a mole fraction in the troposphere of 4%. The C₂H₆ production rate is half the H₂ production rate, implying a net flux to the surface of $2.7 \times 10^9 \text{ cm}^{-2} \text{ s}^{-1}$ (Wilson and Atreya, 2004). Assuming constant production over 4.5 Byr implies an amount of C₂H₆ equivalent to a global liquid ocean 0.7 km deep, consistent with previous estimates.

Further analysis is required to settle the ambiguity between the eddy diffusion coefficient and CH₄ escape flux. If a significant upward flux does exist it cannot be due to thermal escape of CH₄. The Jeans escape rate of CH₄ at 148 K is $0.3 \text{ cm}^{-2} \text{ s}^{-1}$,

which is negligible. However, the H_2 escape rate is clearly in excess of the thermal value. If this difference is due to nonthermal mechanisms for H_2 escape, it suggests that there may be nonthermal contributions to the CH_4 rate as well. CH_4 is 3 times more abundant than H_2 at the exobase, but its scale height is 8 times smaller. Thus, the abundance of CH_4 in the exosphere is roughly 3 times smaller than H_2 . If we assume (questionably) that whatever escape process occurring in the exosphere is mass independent then the CH_4 escape rate should be one third the nonthermal H_2 escape rate, or $\sim 3 \times 10^9 \text{ cm}^{-2} \text{ s}^{-1}$, more than sufficient to alter the derived eddy coefficient. However, it is possible that escape processes operating in the exosphere favor H_2 over CH_4 because of its smaller mass. A detailed examination of neutral and ion densities in the exosphere is necessary to settle this question.

We note that the inferred escape flux depends on the mole fraction of the escaping constituent rather than the number density and therefore depends on the relative calibration of different mass channels but not on the absolute calibration. Our calculation of the Jeans escape flux relies on the number density and therefore does depend on the absolute calibration. Thus, any uncertainties in absolute calibration affect the comparison of the escape flux to the Jeans escape flux, but not the derived values of the escape flux.

The measurements presented here are a snap shot at a particular time over a limited region of Titan's upper atmosphere. Variations in latitude and local time are likely an important component of the structure of Titan's upper atmosphere. The information from this first encounter is that the global variations in Titan's upper atmosphere are quite different from what we expected. The local time variations are opposite to that expected for a solar-driven atmosphere and the exospheric temperature shows no variation with solar cycle. Moreover, it is likely that nonthermal escape processes, presumably magnetospheric in origin, may be responsible for a large fraction of the H_2 escape flux. Thus, further progress in our understanding of Titan's upper atmosphere require more complete measurements of latitude and local time variations and comparison of INMS data with measurements of energetic charged particle distributions in the vicinity of Titan.

Acknowledgments

This research has been supported by the NASA grant NAG5-12699 to the University of Arizona. We thank Allan Lee for supplying the data on Cassini thruster firing shown in Fig. 4.

Appendix A

We derive the diffusion equation for a binary gas mixture with constituents of comparable abundance. The molecular diffusion velocities are related to the mole fractions by Eq. (8.4.7) from Chapman and Cowling (1970),

$$w_1^D - w_2^D = \frac{D_{12}}{X_1 X_2} \left(\frac{\partial X_1}{\partial r} + \frac{(m_1 - m_2)g}{kT} X_1 X_2 \right), \quad (\text{A.1})$$

where w_1^D and w_2^D are the diffusive velocities of species 1 and 2. The diffusion velocities are defined to satisfy mass balance

$$m_1 X_1 w_1^D + m_2 X_2 w_2^D = 0. \quad (\text{A.2})$$

Substitution of (A.2) into (A.1) and using $X_2 = 1 - X_1$ gives

$$\begin{aligned} & \left(1 + \frac{m_1}{m_2} \frac{X_1}{1 - X_1} \right) w_1^D \\ &= - \frac{D_{12}}{X_1(1 - X_1)} \left(\frac{\partial X_1}{\partial r} + \frac{(m_1 - m_2)g}{kT} X_1 X_2 \right), \end{aligned} \quad (\text{A.3})$$

or, solving for w_1^D ,

$$\begin{aligned} w_1^D &= - \frac{D_{12}}{1 - (1 - m_1/m_2)X_1} \\ &\times \left(\frac{1}{X_1} \frac{\partial X_1}{\partial r} + \frac{(m_1 - m_2)g}{kT} (1 - X_1) \right). \end{aligned} \quad (\text{A.4})$$

Defining the eddy diffusion velocity in the usual way

$$w_1^K = -K \frac{1}{X_1} \frac{\partial X_1}{\partial r}, \quad (\text{A.5})$$

and further defining an effective diffusion coefficient by

$$\widetilde{D}_{12} = \frac{D_{12}}{1 - (1 - m_1/m_2)X_1} \quad (\text{A.6})$$

we obtain

$$\begin{aligned} w_1 &= -\widetilde{D}_{12} \left(\frac{1}{X_1} \frac{\partial X_1}{\partial r} + \frac{(m_1 - m_2)g}{kT} (1 - X_1) \right) \\ &\quad - K \frac{1}{X_1} \frac{\partial X_1}{\partial r}. \end{aligned} \quad (\text{A.7})$$

Multiplying by the density gives the flux

$$\begin{aligned} \Phi_1 &= -(\widetilde{D}_{12} + K)N \frac{\partial X_1}{\partial r} \\ &\quad - \widetilde{D}_{12} \frac{(m_1 - m_2)g}{kT} X_1(1 - X_1), \end{aligned} \quad (\text{A.8})$$

which is Eq. (1) in the text.

The formulation above differs from that given in some standard texts [e.g., Banks and Kockarts, 1973, Eq. (15.7)], because those authors based their derivation on the balance of the diffusive number flux, rather than the diffusive mass flux, i.e.

$$X_1 w_1^D + X_2 w_2^D = 0, \quad (\text{A.9})$$

which is incorrect. The result of this error is the appearance of the usual diffusion coefficient, D_{12} , rather than our effective diffusion coefficient, \widetilde{D}_{12} , in Eq. (A.6). \widetilde{D}_{12} could be a factor of two or more greater than D_{12} for diffusion of a light species through a heavy species with comparable abundance.

References

- Banks, P.M., Kockarts, G., 1973. *Aeronomy*. Academic Press, New York/London.
- Bertaux, J.-L., Kockarts, G., 1983. Distribution of molecular hydrogen in the atmosphere of Titan. *J. Geophys. Res.* A 88, 8716–8720.

- Chapman, S., Cowling, C., 1970. *The Mathematical Theory of Non-Uniform Gases*, third ed. Cambridge Univ. Press, Cambridge, UK.
- Flasar, F.M., Achterberg, R.K., Conrath, B.J., Gierasch, P.J., Kunde, V.G., Nixon, C.A., Bjorker, G.L., Jennings, D.E., Romani, P.N., Simon-Miller, A.A., Bézard, B., Coustenis, A., Irwin, P.G.J., Teanby, N.A., Brasunas, J., Pearl, J.C., Segura, M.E., Carlson, R.C., Mamoutkine, A., Schinder, P.J., Barucci, A., Courtin, R., Fouchet, T., Gautier, D., Lellouch, E., Marten, A., Prange, R., Vinatier, S., Strobel, D.F., Calcutt, S.B., Read, P.L., Tayler, F.W., Bowles, N., Samuelson, R.E., Orton, G.S., Spilker, L.J., Owen, T.C., Spencer, J.R., Showlater, M.R., Ferrari, C., Abbas, M.M., Raulin, F., Edgington, S., Ade, P., Wishnow, E.H., 2005. Titan's atmospheric temperatures, winds, and composition. *Science* 308, 975–978.
- Hunten, D.M., 1973. The escape of H₂ from Titan. *J. Atmos. Sci.* 30, 726–732.
- Hunten, D.M., 1982. Thermal and nonthermal escape mechanisms for terrestrial bodies. *Planet. Space Sci.* 30, 773–783.
- Lara, L.M., Lellouch, E., Lopez-Moreno, J.J., Rodrigo, R., 1996. Vertical distributions of Titan's atmospheric neutral constituents. *J. Geophys. Res.* 101, 23261–23283.
- Lebonnois, S., Bakes, E.L.O., McKay, C.P., 2003. Atomic and molecular hydrogen budget in Titan's atmosphere. *Icarus* 161, 474–485.
- Mason, E.A., Marrero, T.R., 1970. The diffusion of atoms and molecules. In: Bates, D.R., Esterman, I. (Eds.), *Advances in Atomic and Molecular Physics*. Academic Press, San Diego, CA, pp. 155–232.
- Müller-Wodarg, I.C.F., Yelle, R.V., 2002. The effect of dynamics on the composition of Titan's upper atmosphere. *Geophys. Res. Lett.* 29, 2139–2142.
- Müller-Wodarg, I.C.F., Yelle, R.V., Mendillo, M., Aylward, A.D., 2003. On the global distribution of neutral gases in Titan's upper atmosphere and its effect on the thermal structure. *J. Geophys. Res.* 108, doi:10.1029/2003JA010054.
- Samuelson, R.E., Nath, N.R., Borysow, A., 1997. Gaseous abundances and methane supersaturation in Titan's troposphere. *Planet. Space Sci.* 45, 959–980.
- Shematovich, V.I., Johnson, R.E., Michael, M., Luhmann, J.G., 2003. Nitrogen loss from Titan. *Icarus* 108, 6–11.
- Smith, G.R., Strobel, D.F., Broadfoot, A.L., Sandel, B.R., Sandel, D.E., Shemansky, D.E., Holberg, J.B., 1982. Titan's upper atmosphere: Composition and temperature from the EUV solar occultation results. *J. Geophys. Res.* 87, 1351–1359.
- Strobel, D.F., Summers, M.E., Zhu, X., 1992. Titan's upper atmosphere: Structure and ultraviolet emissions. *Icarus* 100, 512–526.
- Tobiska, W.K., 2004. SOLAR2000, modeled solar irradiances, solar proxies, aeronomy, space system operations. *Adv. Space Res.* 34, 1736–1746.
- Toublanc, D., Parisot, J.P., Briller, J., Gautier, D., Raulin, F., McKay, C.P., 1995. Photochemical modeling of Titan's atmosphere. *Icarus* 113, 2–26.
- Vervack Jr., R.J., Sandel, B.R., Strobel, D.F., 2004. New perspectives on Titan's upper atmosphere from a reanalysis of the Voyager 1 UVS solar occultations. *Icarus* 170, 91–112.
- Waite, J.H., Lewis, W.S., Kasprzak, W.T., Anicich, V.G., Block, B.P., Cravens, T.E., Fletcher, G.G., Ip, W.-H., Luhmann, J.G., McNutt, R.L., Niemann, H.B., Parejko, J.K., Richards, J.E., Thorpe, R.L., Walter, E.M., Yelle, R.V., 2005. The Cassini Ion and Neutral Mass Spectrometer (INMS) investigation. *Space Sci. Rev.* 114, 113–231.
- Wilson, E.H., Atreya, S.K., 2004. Current state of modeling the photochemistry of Titan's mutually dependent atmosphere and ionosphere. *J. Geophys. Res.* 109, doi:10.1029/2003JE002181.
- Yelle, R.V., 1991. Non-LTE models of Titan's upper atmosphere. *Astrophys. J.* 383, 380–400.
- Yung, Y.-L., Allen, M., Pinto, J.P., 1984. Photochemistry of the atmosphere of Titan: Comparison between model and observations. *Astrophys. J. Suppl.* 55, 465–506.